AD-A040 459 ATLANTIC RESEARCH CORP ALEXANDRIA VA KINETICS AND CO--ETC F/G 21/9.2
A MODEL OF EROSIVE BURNING OF COMPOSITE PROPELLANTS,(U)
1977 M K KING F44620-76-C-0023

UNCLASSIFIED AFOSR-TR-77-0692 NL

| OF |
AD
A040 459

END

DATE
FILMED
7-77

A MODEL OF EROSIVE BURNING OF COMPOSITE PROPELLANTS*

Dr. Merrill K. King**
Atlantic Research Corporation
Alexandria, Virginia 22314

Abstract

Development of solid rocket motor designs which result in high velocity flows of product gases across burning propellant surfaces (notably, nozzleless rocket motors) is leading to increased occurrence of erosive burning. In this paper, a physically realistic picture of the effect of such crossflows on composite propellant combustion, based on the bending of columnar diffusion flames by the crossflow, is presented. This bending results in shifting of the diffusion flame heat release zone toward the surface, with consequent increased heat feedback flux from this flame to the surface and thus increased burning rate. A relatively simple analytical model based on this picture is developed for prediction of propellant burning rate as a function of pressure and crossflow velocity, given only zero-crossflow burning rate versus pressure data. Model predictions and experimental results are compared, with reasonably good agreement being found.

Introduction

Requirements for ever higher propellant loading fractions in solid propellant rocket motors and for higher thrust-to-weight ratios have led to development of centrally perforated grain configurations with relatively low port-to-throat area ratios. This, in turn, results in high velocities of propellant gases across burning propellant surfaces in the aft portions of these grains, leading to erosive burning. Moreover, a series of studies has demonstrated that the nozzleless rocket concept offers significant economic advantages over a more conventional rocket system when considered for some tactical weapon systems. This concept requires that the flow within the bore or central perforation of a grain accelerate to the point that sonic conditions are achieved at the aft end. In this situation, the high velocity environment leads to a realm of erosive burning not previously considered. The effects are critical in that the erosive burn rate contributions strongly influence performance level, performance repeatability and thrust misalignment. More than in any conventional motor, the exact erosive burn rate behavior must be held constant from batch to batch if reproducibility is not to be a problem. The performance sensitivity of a nozzleless motor to erosion is due to the fact that the maximum erosion occurs at the choke point in the base. Since this point is the effective throat area, and the throat area versus time is thus a function of regression rate, the result is a chamber pressure history which varies strongly with erosion.

In a nozzleless motor, two parameters which affect burning rate, pressure and crossflow velocity, vary strongly from the fore end to the aft end of the grain, static pressure decreasing and crossflow velocity increasing with distance from the head end of the grain. Assuming that an erosive burning rate expression of the form, $r/r_o = 1 + k_3 M$, is applicable (with $r_o = bp^n$), it may be shown[1] that for constant port area along the grain:

$$r_{aft}/r_{fore} = (k_3+1)/(\gamma + 1)^n \qquad (1)$$

Values of $(r_{aft}/r_{fore})_{initial}$ as a function of the erosivity constant (k_3) and the burning rate exponent (n) are presented in Table I for $\gamma = 1.25$. As may be seen, for the case of no erosion ($k_3 = 0$) the aft end will recede more slowly than the fore end, due to lower pressure at the aft end. As k_3 increases, the r_{aft}/r_{fore} ratio also increases, going through unity (generally desirable) at a value of k_3 which depends on the burning rate exponent. The results of Table I give some indication of the sensitivity of nozzleless motor design to the erosive burning characteristics of the propellant and thus point out the importance of information regarding the propellant's erosive burning characteristics to the designer.

Table I. Ballistic Analysis of a Nozzleless Motor with Uniform Port Area.

$r/r_o = 1 + k_3 M$, $r_o = bp^n$

n	k_3	r_{AFT}/r_{FORE}
0.4	0	0.72
	0.5	1.08
	1.0	1.45
	1.5	1.80
0.6	0	0.61
	0.5	0.92
	1.0	1.23
	1.5	1.54
0.8	0	0.52
	0.5	0.78
	1.0	1.05
	1.5	1.31

Development of a better understanding of the effects of crossflows on solid propellant combustion is needed for accomplishment of accurate motor performance predictions in terms of both mean interior ballistics analysis and prediction of motor stability characteristics. With such understanding, the motor designer can either design his grains to compensate for mean erosive burning effects on grain burn pattern, or, knowing how propellant formulation parameters affect erosion sensitivity, vary propellant parameters in such a way as to optimize these effects. A review of the literature indicates that there is no unifying predictive model for erosive burning of solid propellants.

General observations of importance from past experimental studies[2-11] include:

1. Plots of burning rate versus gas velocity or mass flux at constant pressure are usually not fitted best by a straight line.
2. Threshold velocities and "negative" erosion rates are often observed.
3. Slower burning propellants are more strongly

*This effort was supported by AFOSR under Contract No. F44620-76-C-0023, monitored by Maj. Thomas Meier
**Chief Scientist, Research & Technology, Member AIAA

AIR FORCE OFFICE OF SCIENTIFIC RESEARCH (AFSC)
NOTICE OF TRANSMITTAL TO DDC
This technical report has been reviewed and is
approved for public release IAW AFR 190-12 (7b).
Distribution is unlimited.
A. D. BLOSE
Technical Information Officer

affected by crossflows than higher burning-rate formulations.

4. At high pressure, the burning rate under erosive conditions tends to approach the same value for all propellants (at the same flow velocity) regardless of the burning rate of the propellants at zero crossflow.
5. Erosive burning rates do not depend upon gas temperature of the crossflow (determined from tests in which various "driver propellants" products are flowed across a given test propellant).

There is, however, very little data available for high crossflow velocities (greater than $M \approx 0.3$). In addition, there has been no study in which various propellant parameters have been systematically varied one at a time. Such a study is necessary for determination of erosive burning mechanisms and proper modeling of the erosive burning phenomena. Much of the past work has not resulted in instantaneous (as opposed to averaged over a range of pressure and crossflow velocity) measurements of erosive burning rates under well characterized local flow conditions.

From the above discussion, it is apparent that development of an analytical model of erosive burning, properly describing the physical effects which result in augmentation of solid composite propellant burning rate by crossflows, coupled with an experimental effort to systematically define the effects of various formulation parameters on erosive burning at crossflow velocities up to Mach 1 is of great importance to the design and development of advanced solid rocket systems.

Background: Existing Models

The objectives of a theoretical model of erosive burning are to provide a means of predicting the sensitivity of propellant combustion rate to gas flow parallel to the ablating surface and to indicate what effect various formulation parameters have on this sensitivity. An acceptable model must account for: (1) any effects observed when crossflow gas temperature is varied; (2) observed pressure dependency; and (3) nullification of catalyst activity under erosive conditions. This model should provide an explanation of the observed behavior in terms of the hydrodynamic conditions induced by a crossflow coupled with the chemical and physical processes that constitute the propellant deflagration mechanism.

Over the years, a large number of erosive burning models, of varying degrees of sophistication, have been developed - a list of models examined by this author is presented as Table II. These models generally fall into one of three categories, as indicated. The first category is based on the assumption that the erosive burning is driven by increased heat transfer from the mainstream gas flow associated with increased heat transfer coefficient with increased mass flux parallel to the grain surface. The best-known and most widely used erosive burning model, that of Lenoir and Robillard[12], falls into this category. In this model, the authors calculate the total burning rate (r) as the sum of the normal (no crossflow) burning rate and a second erosive term resulting from heat transfer from the "core" flow to the propellant surface. This equation entails an a priori assumption that the pressure-dependent "base" rate (r_o) is unaffected by an increase in total rate at a given pressure, very unlikely within the constraints of other assumptions in the model. This problem has been discussed in detail by King[28], with derivation of a modified Lenoir and Robillard expression allowing for the coupling of flame standoff distance with burning rate. While Lenoir and Robillard assume $r = r_o + r_e$, allowance for this coupling results in $r = (r_o^2/r) + r_e$. In physical terms, Lenoir and Robillard have failed to account for the fact that increased burning rate, caused by erosive feedback at constant pressure, results in the propellant flame being pushed further from the surface, decreasing its heat feedback rate, and thus decreasing the propellant burning rate part of the way back toward the base rate.

Table II. General Types of Models of Erosive Burning Developed to Date.

1. MODELS BASED ON HEAT TRANSFER FROM A "CORE GAS" IN THE PRESENCE OF CROSS FLOW
   - LENOIR & ROBILLARD (12)
   - BURICK AND OSBORN (13)
   - ZUCROW, OSBORN AND MURPHY (14)
   - SADERHOLM (3)
   - MARKLUND (8)
   - JOJIC & BLAGOJEVIC (15)
2. MODELS BASED ON ALTERATION OF TRANSPORT PROPERTIES IN REGION FROM SURFACE TO FLAME ZONE BY CROSSFLOW, GENERALLY DUE TO TURBULENCE EFFECTS. INCLUDES EFFECTS ON CONDUCTIVITY FROM FLAME ZONE BACK TO PROPELLANT AND EFFECTS ON TIME FOR CONSUMPTION OF FUEL POCKETS LEAVING SURFACE.
   - SADERHOLM, BIDDLE, CAVENY, et al (16)
   - LENGELLÉ (17)
   - CORNER (DOUBLE-BASE) (18)
   - VANDENKERCKHOVE (DOUBLE-BASE) (19)
   - ZELDOVICH (DOUBLE-BASE) (20)
   - VILYUNOV (DOUBLE-BASE) (11)
   - GECKLER (21)
3. MODELS BASED ON CHEMICALLY REACTING BOUNDARY LAYER THEORY (HOMOGENEOUS SYSTEMS ONLY)
   - TSUJI (22)
   - BEDDINI, et al (23)
   - KUO, et al (24)
4. OTHER
   - KLIMOV (25)
   - MOLNAR (26)
   - MILLER (27)
   - KING

A more general weakness of models in the first category is that these models predict substantial dependence on the temperature of the core gas: such dependence was found by Marklund and Lake[8] to be completely absent. Analysis of the Lenoir and Robillard treatment indicates that the erosive contribution to burning rate (r_e) is given by:

$$r_e \propto G^{0.8}\, \mu_{gas}^{0.2}\, (T_{core\ gas} - T_s). \qquad (2)$$

for a given test propellant and geometry. But, at fixed crossflow velocity and pressure, G is inversly proportional to the core gas (driver propellant products) temperature while μ_{gas} is roughly directly proportional to this temperature. Therefore,

$$r_e \propto T_{core\ gas}^{-0.6}\, (T_{core,gas} - T_s). \qquad (3)$$

However, Marklund and Lake performed a set of experiments in which crossflow velocity and pressure were held constant while the driver propellant was changed from a 1700°K propellant to a 2500°K propellant, with T_s being approximately 800°K in both cases. Thus, the Lenoir and Robillard theory would indicate that:

$$\frac{r_{e,\ 2500°K\ driver}}{r_{e,\ 1700°K\ driver}} = \frac{1700}{900}\left(\frac{2500}{1700}\right)^{-0.6} = 1.50 \quad (4)$$

That is, with the higher driver gas temperature case, the erosive burning rate component of the total burning rate should be 50 percent higher than that for the low driver gas temperature. However, as mentioned, Marklund and Lake observed no difference in erosive rates in the two cases. This observed lack of dependence of the erosive burning rate on core gas temperature tends to cast doubt on all models in the first category of Table II.

The second category of models listed in Table II includes models based upon the alteration of transport properties in the region between the gas flame and the propellant surface by the crossflow, generally due to turbulence effects. Included in this category are models in which the thermal conductivity in this region is raised by turbulence and models in which the time for consumption of fuel gas pockets leaving the surface is reduced by the effects of turbulence on diffusivity. Four of these models were developed for double-base propellants as indicated, and will not be reviewed here. Of the composite propellant models in this category, that of Lengelle[17] appears to be the most advanced. The basic propellant combustion mechanism assumed is the granular diffusion model in which pockets of fuel vapor leave the surface and burn away in an oxidizer continuum at a rate strongly dependent upon the rate of micromixing of the oxidizer vapor into the fuel vapor pocket. The driving mechanism by which the crossflow is assumed to increase the burning rate is through increased turbulence associated with increasing crossflow raising the turbulent diffusivity in the mixing region (thus increasing the rate of mixing of the binder and oxidizer product gases) and raising the effective turbulent thermal conductivity. The increase in thermal conductivity increases the heat transfer rate from the flame to the surface, while the increase in mixing rate just offsets the increase in gas velocity away from the surface, with the result that the flame offset distance remains constant. There are several weaknesses associated with the Lengelle model: (1) the granular diffusion flame model is not physically realistic; (2) the ammonium perchlorate monopropellant flame is ignored; and (3) the boundary layer treatment used to calculate the dependence of the effective turbulent diffusivity and conductivity on the crossflow is unrealistic in its use of a 1/7th power velocity law all the way from the free-stream to the surface.

Of the three models listed in the third category (models based on chemically reacting boundary layer theory) one is complete, while the remaining two are in development. The completed model, by Tsuji[22], is unfortunately not particularly useful due to the assumption of a totally laminar boundary layer and limitation to a situation where the free-stream velocity is proportional to the distance from the head-end of the grain. Other simplifications include assumption of premixed stoichiometric fuel and oxidizer (rendering the model inapplicable to composite propellant systems) and use of one-step global kinetics.

In the model of Beddini, et al[23], primary emphasis is placed on analysis of a well-developed turbulent flow field in a propellant grain port for definition of turbulent transport of heat, mass, and momentum in the boundary layer. An extended version of the second-order closure method of Donaldson is used to calculate the details of the turbulent flow field. To date, this flow field analysis has been coupled only with a very simple model of propellant combustion in which the propellant surface temperature is assumed to be independent of burning rate, the mass burning rate is assumed to be directly proportional to the heat flux from the gas to the surface, and the gas phase reaction is assumed to be described by a single step homogeneous reaction which is first order with respect to fuel concentration and first order with respect to oxidizer concentration. Under these conditions, the model predicts a threshold velocity for erosion followed by a quasi-linear dependence of burning rate on crossflow velocity due to turbulence entering the propellant flame zone.

Kuo and Razdan[24] are also using a second-order turbulence closure model for characterization of the flow field in erosive burning situations, the closure model being used differing from that being used by Beddini. In addition, postulated flame mechanisms (the details of which are unknown to this author) for composite propellants are being coupled into the analysis. At this time, the governing equations have been developed and boundary conditions defined, but the equation solving procedure has not been completed.

The Klimov model[25] is mainly aimed at calculation of threshold crossflow velocities (below which the propellant is unaffected by crossflow). Klimov claims that the threshold velocity is the main stream crossflow velocity above which the "turbulence front" subsides onto the propellant surface, and presents boundary layer analysis procedures for calculating this threshold velocity as a function of the transpiration (blowing) velocity of the gases ablating from the propellant surface. In addition, he postulates that negative erosion (sometimes seen at low crossflow velocities) is due to the "sitrring up" of cool streams of binder decomposition products over the oxidizer surface, leading to intensification of their cooling effect and to screening of heat feedback from the diffusion flame.

Molnar's model[26], developed for homogeneous propellants with a laminar crossflow, is based on an assumption (which does not appear to this author to be substantiated) that the lateral velocity gradient at the burning surface governs erosive burning. Miller[27] assumes that the time for a unit of propellant to be consumed is a linear sum of a chemical reaction time and "the time required for turbulent transport of heat to the propellant surface" - such an additivity approach does not appear to this author to be physically realistic.

Of the models briefly discussed above, those of Lengelle[17], Beddini, et al[23], and Kuo and Razdan[24] appear to be the most advanced (although it is not clear at this time how the latter two teams will build the complex heterogeneous flame structure associated with composite propellant combustion into their fluid dynamic boundary layer treatments). Common to all three of these models is the assumption that the increase in propellant burning rate associated with crossflow results from turbulence associated with this crossflow penetrating between the propellant gas flame zone(s) and the surface, causing increases in mass and energy transport rates. However, for a typical propellant containing oxidizer

particles with diameters of from 10 to 50 μm, diffusion flame offset distances may be calculated to be typically of the order of one-quarter to one-half of the particle diameter or 2.5 to 25 μm. On the other hand, for a crossflow velocity of 200 m/s (650 ft/sec), the universal u^+, y^+ correlation (transpiration effects neglected) indicates a laminar sublayer thickness of approximately 10 μm and a buffer zone of approximately 50 μm, full turbulence not being achieved closer than 60 μm from the propellant surface. Moreover, transpiration of the binder and oxidizer decomposition gases from the propellant surface will tend to increase the thickness of these zones. Thus it is not at all certain that crossflow-induced turbulence does penetrate into the zone between the propellant surface and the gas phase flame zone(s). In addition, even if the turbulent region does extend into this zone, in order for the eddies to have significant effect on mixing and thus on heat and mass transfer, they must be considerably smaller than the flame offset distance - that is, they must be on the order of 1 μm in diameter or less. It is not at all clear to this author that a significant degree of turbulence of this scale will be induced in the zone between the propellant surface and the gas phase flame zone(s) by crossflows even up to Mach 1, more than an order of magnitude above typical erosive burning threshold velocities. Accordingly an alternate possible mechanism for erosive burning of composite propellants is presented below.

Model Development

In development of a proper model of erosive burning, it is necessary that a physical-chemical mechanism for the "normal" (no crossflow) burning of such propellants be specified, that the boundary layer flow be properly described (theoretically or empirically) and that the descriptions of these processes be properly coupled.

Considering first the flow field, it is informative to estimate flow profiles and angles near the surface of a composite propellant for a typical erosive burning situation. As an example, let us examine a case where the operating pressure is 6.89 (10^6) N/m^2 (1000 psi), the propellant flame temperature is 3000 °K, the crossflow mainstream velocity is 200 m/sec (650 ft/sec), the characteristic length dimension for determining Reynold's Number is 15 cm (0.5 feet) and the propellant burning rate is 1.25 cm/sec (0.5 in/sec). In this case, the gas velocity away from the surface at the flame temperature is approximately 4 m/sec (13 ft/sec). Using Mickley and Davis[29] flow profile data for boundary layer profiles in the presence of transpiration, we estimate that the crossflow velocity 10 μm from the propellant surface is about 10 m/sec (30 ft/sec). A simplified energy balance equating the heat feedback flux from a flame sheet above a propellant surface to the value required for preheating and vaporizing the solid ingredients at a regression rate of 1.25 cm/sec (0.5 in/sec) indicates that the gas-phase flame must be on the order of 10 μm from the surface. Thus, at the position of the gas-phase flame front, the velocity component away from the propellant is about 4 m/sec while the velocity component parallel to the surface is 10 m/sec, and the resultant flow vector makes an angle with the propellant surface of only 22 degrees. While this vector will vary with distance from the surface, since the velocity components normal to and parallel to the surface do not scale with distance from the surface in exactly the same way, the variation will not be great. Thus fuel and oxidizer gas columns leaving the surface will not flow perpendicular to the surface (as they would in the absence of crossflow) but at an angle of approximately 20 to 25 degrees from parallel with the surface.

The important feature of this picture is that any diffusion flame at the AP-binder boundaries is bent over toward the propellant surface by the crossflow velocity. Since the deflection of this mixing column or cone can be shown to cause the distance from the base to the tip, measured perpendicular to the base, to decrease, the height above the propellant at which any given fraction of the mixing of AP products and fuel decomposition products is complete should, therefore, be decreased and the distance from the propellant surface to the "average" location of the diffusion flame should also be decreased. This, in turn, will increase heat feedback and thus increase burning rate. The schematic of a composite propellant erosive burning model based upon this picture is shown in Figure 1.

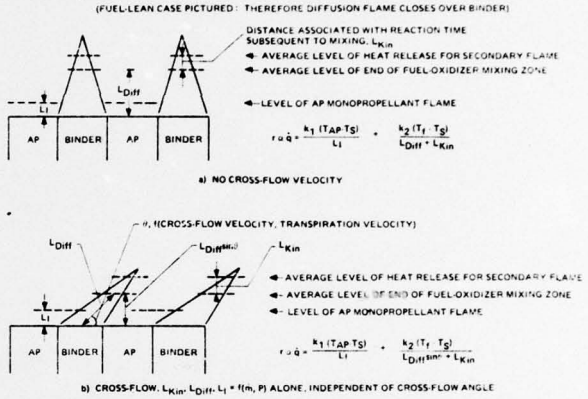

Figure 1. Schematic of Geometrical Model of Erosive Burning (Two-Flame Model).

In the first part of the figure, the flame processes occurring in the absence of crossflow are depicted. There are two flames considered, an ammonium perchlorate deflagration monopropellant flame close to the surface and a columnar diffusion flame resulting from mixing and combustion of the AP deflagration products and fuel binder pyrolysis products at an average distance somewhat further from the surface. Three important distance parameters considered are the distance from the propellant surface to the "average" location of the kinetically controlled AP monopropellant heat release (L_I), the distance associated with mixing of the oxidizer and fuel for the diffusion flame (L_{Diff}), and the distance associated with the fuel-oxidizer reaction time subsequent to mixing (L_{Kin}). A heat balance between heat feedback from these two flames and the energy requirements for heating the propellant from its initial temperature to the burning surface temperature and decomposing it yields (assuming that the heat feedback required per unit mass of propellant consumed is independent of burning rate):

$$r \propto \dot{q}_{feedback} \propto \frac{k_1 (T_{AP} - T_s)}{L_I} + \frac{k_2 (T_f - T_s)}{L_{Diff} + L_{Kin}} \qquad (5)$$

The situation pictured as prevailing with a cross flow is shown in the second part of Figure 1. Since L_I and L_{Kin} are both kinetically controlled and are thus simply proportional to a characteristic reaction time (which is assumed to be unaffected by the

crossflow) multiplied by the propellant gas velocity normal to the surface (which for a given formulation is fixed by burning rate and pressure alone) these distances are fixed for a given formulation at a given burning rate and pressure, independent of the crossflow velocity. Of course, since crossflow velocity affects burning rate at a given pressure through its influence on the diffusion process as discussed below, L_I and L_{Kin} are influenced through the change in burning rate, but this is simply coupled into a model by expressing L_I and L_{Kin} as explicit functions of burning rate and pressure in that model. The important point is that they can be expressed as functions of these two parameters alone for a given propellant. However, the distance of the mixing zone from the propellant surface is directly affected by the crossflow. It may be shown through geometrical arguments coupled with the columnar diffusion flame height analysis presented by Schultz, Penner and Green[5], that L_{Diff} measured along a vector coincident with the resultant crossflow and transpiration velocities should be approximately the same as L_{Diff} in the absence of a crossflow at the same burning rate and pressure (except at very high ratios of local crossflow velocity to transpiration velocity). That is, the magnitude of L_{Diff} is essentially independent of the crossflow velocity, although its orientation is not. Thus, the distance from the surface to the "average" mixed region is decreased to $L_{Diff} \sin \theta$ where θ represents the angle between the surface and the average flow vector in the mixing region. The heat balance at the propellant surface now yields:

$$r \propto \dot{q}_{feedback} \propto \frac{k_1(T_{AP} - T_s)}{L_I} + \frac{k_2(T_f - T_s)}{L_{Diff} \sin \theta + L_{Kin}} \qquad (6)$$

This picture has been used as the basis of development of a model for prediction of burning-rate versus pressure curves at various crossflow velocities, given only a curve of burning rate versus pressure in the absence of crossflow. This model employs no empirical constants other than those obtained from regression analysis of the no-crossflow burning rate data. Thus, although it is not as powerful as a model which would permit prediction of erosive burning phenomena with no burning rate data at all, but only propellant composition and ingredient size data, it is still a very useful tool in that it permits prediction of erosive burning characteristics given only relatively easily obtained strand-bomb burning rate data. (By comparison, the Lenoir and Robillard model employs two free constants which are adjusted to provide a best fit of erosive burning data for a given propellant and since since these constants vary from propellant to propellant, the Lenoir and Robillard model does not permit a *priori* erosive burning predictions for new propellants without some erosive burning data, where as the model presented here does not require such data.)

The general approach followed in development of this model is:

1. The expressions for L_I, L_{Diff}, and L_{Kin} as functions of burning rate (or burning mass flux, $\dot{m}$), pressure, and propellant properties are derived and substituted into a propellant surface heat balance.
2. The resulting equation is worked into the form (developed in succeeding paragraphs):

$$r = A_3 P \left[1 + \frac{A_4}{1 + A_5 d_p^2 P^2} \right]^{1/2} \qquad (7)$$

for burning in the absence of crossflow. A regression analysis using no-crossflow burning rate data is performed to obtain best fit values for A_3, A_4, and A_5. (d_p is the average ammonium perchlorate particle size. For a given propellant, the burning rate data may be just as effectively regressed on A_3, A_4, and $A_5 d_p^2$, eliminating the necessity of actually defining an effective average particle size.)

3. From these results, expressions are obtained for L_I, L_{Diff}, and L_{Kin} as functions of burning rate (or $\dot{m}$) and pressure.
4. These expressions are combined with an analysis of the boundary layer flow (which gives the crossflow velocity as a function of distance from the propellant surface, mainstream velocity, and propellant burning rate) to permit calculation of the angle θ (Figure 1), L_I, L_{Diff}, L_{Kin}, and $\dot{m}$ for a given pressure and crossflow velocity.

In the derivation of a burning rate expression for a composite propellant in the absence of a crossflow, an energy balance at the propellant surface is first written as: (See Figure 1.)

$$\frac{\lambda_A(T_f - T_s)}{(L_{Diff}) + (L_{Kin})} + \frac{\lambda_B(T_{AP} - T_s)}{L_I} = \dot{m}[C_p(T_s - T_o) + Q_{VAP} - Q_{RX}] \qquad (8)$$

The first term of this equation represents heat flux from the final flame to the surface, the second represents heat flux from the AP monopropellant flame, and the third represents the heat flux requirements for ablation of the propellant at the mass flux, $\dot{m}$. Several simplifying assumptions are obviously involved in writing of the equation in this form. Probably the most important and tenuous of these is the assumption that Q_{RX} is independent of burning rate (or $\dot{m}$) and of pressure. In the Zeldovich picture of solid propellant combustion, where subsurface exothermic reactions with fairly high activation energies are considered to dominate, this would be a very poor assumption, but in the generally accepted picture of solid propellant combustion in this country, it is not a bad approximation. In addition, it is assumed that the surface temperature is nearly constant with respect to pressure and burning rate, with the resultant uncoupling of this heat balance equation from a surface regression rate Arrenhius expression. Finally, it is assumed that for the diffusion flame, a distance associated with mixing may be added linearly to a distance associated with reaction delay to yield a total flame offset distance, a fairly gross simplification.

The monopropellant AP flame offset distance, L_I, may be expressed as the product of a characteristic reaction time, τ_I, and the linear velocity of gases leaving the propellant surface:

$$L_I = \tau_I \frac{\dot{m}}{\rho_{gas}} \qquad (9)$$

For a second-order gas-phase reaction (generally assumed), τ_I is inversely proportional to pressure, and for a given formulation, the gas density is

directly proportional to pressure, yielding:

$$L_I = K_1 \dot{m}/P^2 \quad (10)$$

A similar analysis for L_{Kin} yields:

$$L_{Kin} = K_2 \dot{m}/P^2 \quad (11)$$

For a columnar diffusion flame, it may easily be shown[30] that the diffusion cone height, L_{Diff}, may be expressed as:

$$L_{Diff} = K_3 \dot{m} d_p^2 \quad (12)$$

Equations 8 and 10 - 12 may be combined to yield:

$$r = \dot{m}/\rho_s = A_3 P \left[1 + \frac{A_4}{1 + A_5 d_p^2 P^2} \right]^{1/2} \quad (13)$$

Burning rate versus pressure data for a given propellant in the absence of a crossflow may then be analyzed via a fairly complicated regression analysis procedure to yield values of the constants A_3, A_4, and A_5 (or $A_5 d_p^2$) for that given propellant. The constants K_1, K_2, and K_3 are related to these constants in turn by:

$$K_1 = \frac{(T_{AP} - T_s)\lambda_B}{A_2 A_3^2 \lambda_A} \quad (14)$$

$$K_2 = \frac{(T_f - T_s)}{A_2 A_3^2 A_4} \quad (15)$$

$$K_3 = \frac{(T_f - T_s)A_5}{A_2 A_3^2 A_4} \quad (16)$$

where:

$$A_2 = \frac{\rho_{prop}^2 [C_p (T_s - T_{bulk}) + Q_{VAP} - Q_{RX}]}{\lambda_A} \quad (17)$$

In this analysis a rough estimate of A_2 has been made to permit calculation of values of K_1, K_2, and K_3 from the best-fit values of A_3, A_4, and A_5. It should be pointed out, however, that the subsequent calculations of burning rates in crossflows are not strongly affected by the estimate of A_2, since the same value of A_2 is used in that analysis, and thus its effects essentially cancel. The value used for most cases (except those cases run to test the effect of A_2) was $2 \cdot 10^6$ gm sec °K/cm^5.

Data of Mickley and Davis[29] were used to develop empirical expressions for the local crossflow velocity as a function of distance from the propellant surface, mainstream crossflow velocity, and transpiration rate (gas velocity normal to the propellant surface). In this analysis, it was decided that the transpiration velocity should be calculated as the gas velocity normal to the surface at the final flame temperature. (Mickley and Davis correlations are based upon the ratio of mainstream velocity to transpiration velocity.) The procedure used is outlined in Table III.

The above analyses were used in the derivation of the following eight equations in eight unknowns for the burning of a given composite propellant at a given pressure and crossflow velocity:

$$r = \frac{K_2'}{L_{Diff} \sin\theta + L_{Kin}} + \frac{K_7'}{L_I} \quad (18)$$

$$L_{Diff} = K_1' r \quad (19)$$

$$L_{Kin} = K_5' r \quad (20)$$

$$L_I = K_6' r \quad (21)$$

$$V_{transpiration} = K_3' r \quad (22)$$

$$Y^+_{y=L_{Diff}\sin\theta} = K_8' r \sin\theta \quad (23)$$

$$U_{Crossflow,\, y=L_{Diff}\sin\theta} = K_9' f(Y^+_{y=L_{Diff}\sin\theta}) \quad (24)$$

$$\sin\theta = \frac{V_{Transpiration}}{\sqrt{V^2_{Transpiration} + U^2_{Crossflow,\, y=L_{Diff}\sin\theta}}} \quad (25)$$

where

$$K_1' = \frac{(T_f - T_s) A_5 d_p^2 \rho_s}{A_2 A_3^2 A_4} \quad (26)$$

$$K_2' = \rho_s (T_f - T_s)/A_2 \quad (27)$$

$$K_3' = \frac{R T_f \rho_s}{P (MW)} \quad (28)$$

$$K_5' = \frac{(T_f - T_s)\rho_s}{A_2 A_3^2 A_4 P^2} \quad (29)$$

$$K_6' = \frac{(T_{AP} - T_s)\rho_s \lambda_B}{A_2 A_3^2 P^2 \lambda_A} \quad (30)$$

$$K_7' = [\rho_s (T_{AP} - T_s)/A_2](\lambda_B/\lambda_A) \quad (31)$$

$$K_8' = \frac{K_1' U^* \rho_{gas,\, T=(T_f + T_s)/2}}{\mu_{gas,\, T=(T_f + T_s/2}} \text{ (See Table III)} \quad (32)$$

$$K_9' = U^* \text{ (See Table III)} \quad (33)$$

and the function f of Equation 24 is given in Table III.

Table III. Calculation of Cross-flow Velocity Profile in Current Erosive Burning Model.

1. NEGLECTING TRANSPIRATION EFFECTS

CALCULATE $U^* = U_{Mainstream}\sqrt{\frac{f}{2}} = \frac{0.152\, U_{Mainstream}}{(Re)^{0.1}}$

$$= \frac{0.023\, (U^{0.9}_{Mainstream})\, (273 + T_f)^{0.18}}{D^{0.1}\, \rho^{0.1}}$$

CALCULATE $Y^+ = Y U^* \rho/u$

CALCULATE $U^+ = Y^+$ FOR $Y^+ < 5$

$U^+ = -3.05 + 5.00$ LN Y^+ FOR $5 < Y^+ < 30$

$U^+ = 5.5 + 2.5$ LN Y^+ FOR $Y^+ > 30$

CALCULATE $U = U^+ U^*$

2. ALLOWING FOR TRANSPIRATION (USING DATA OF MICKLEY AND DAVIS) DO ALL OF THE ABOVE AND CORRECT RESULT BY

$$U_{Transpiration\ Case} = U_{No\ Transpiration} \exp(60\, V_{Transpiration}/U_{Mainstream})$$

Implicit in Equation 25 is the assumption that the transpiration velocity and the crossflow velocity maintain a constant ratio from very near the surface out to the end of the diffusion zone: that is, that the vector resultant is a straight line. This approximation is probably not seriously in error, and should not strongly affect the results

of the calculations.

As may be seen, the quantity A_2 appears in the denominator of K_2', K_7', K_1', K_5', and K_6'. Thus, as indicated earlier, the effect of A_2 in Equation 18 cancels out and the predicted burning rate is dependent upon this parameter only to the extent that it affects the calculation of the crossflow velocity at distance $L_{Diff} \sin \theta$ from the surface. Parametric calculations with various values of A_2 indicate that this effect is very weak. A computer code has been developed to solve these equations simultaneously, yielding a predicted burning rate for a given pressure, crossflow velocity and set of constants A_3, A_4, and $A_5 d_p^2$ obtained from regression analysis of no-crossflow data.

Comparison of Predictions With Data

Original testing of the model was carried out using a systematic erosive burning data set taken by Saderholm[3]. (This was the only systematic data set found in the literature with sufficient zero crossflow data to permit evaluation of A_3, A_4, and $A_5 d_p^2$.) The computer code described above was used to calculate burning rate versus pressure curves for several crossflow velocities studied by Saderholm, with and without correction of the boundary layer profiles for transpiration effects. The results are shown in Figures 2 and 3. As shown in Figure 2, neglecting correction for the effects of transpiration on the boundary layer profile results in serious overprediction of the burning rates. However, as shown in Figure 3, agreement between predictions and data is excellent when the transpiration correction factor is included.

In parallel with this modeling effort, Atlantic Research is carrying out an experimental test program to obtain systematic erosive burning data for a series of propellant formulations. This experimental program is described in some detail in Ref. 1 and 31. At this time, a fairly complete set of data covering a pressure range of 10^6 to 5 (10^6) n/m^2 (10 to 50 atmospheres) and a crossflow velocity range of 200 to 700 m/sec (600 to 2200 ft/sec) have been obtained for one formulation, designated Formulation 4525. This is a "scholastic" formulation, containing unimodal ammonium perchlorate. The

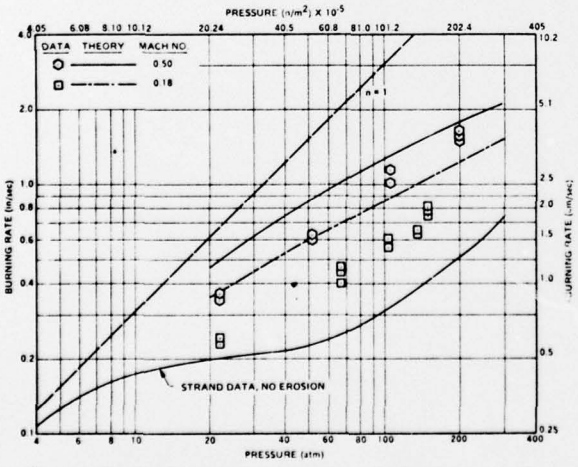

Figure 2. Erosive Burning Model Predictions and Comparisons with Saderholm Data. Transpiration Effects not Included.

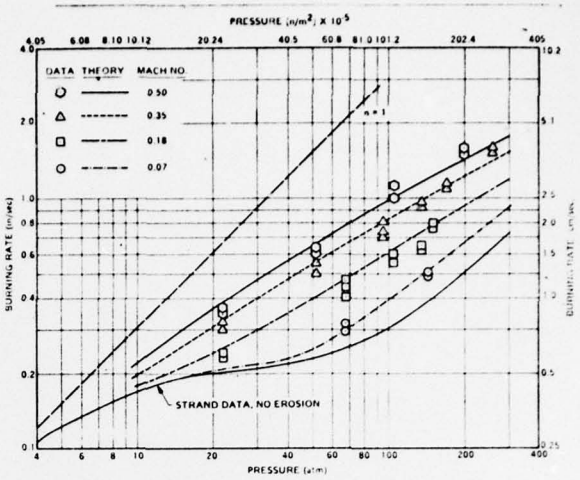

Figure 3. Erosive Burning Model Predictions and Comparisons with Saderholm Data. Transpiration Effects Included.

formulation consists of 73 weight percent 20 micron diameter ammonium perchlorate and 27 weight percent hydroxy terminated polybutadiene (HTPB) binder, with a trace of carbon black added to opacify the propellant. Experimental and theoretical results are presented in Figures 4 and 5. As may be seen, agreement between prediction and data, while not as good as with the Saderholm propellant, is not bad. The predicted curves for burning rate versus pressure at various crossflow velocities (Figure 4) do seem to group more tightly than the data. That is, as shown more clearly in Figure 5, the model tends to overpredict the burning rate at low crossflow velocities and underpredict it at high velocities.

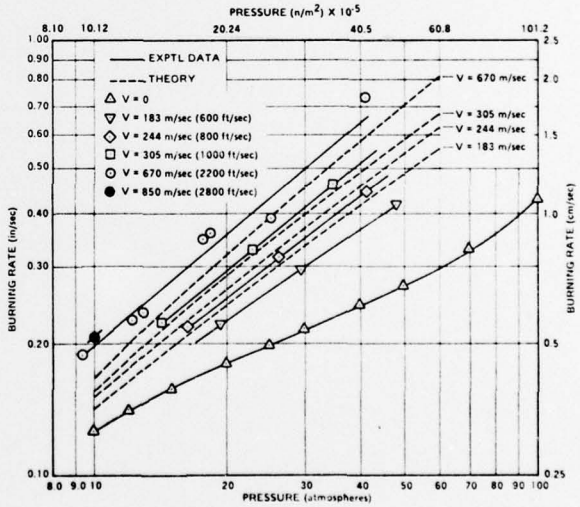

Figure 4. Burning-Rate Versus Pressure Data and Predictions for Various Crossflow Velocities for Formulation 4525 (73/27 AP/HTPB, 20μm AP).

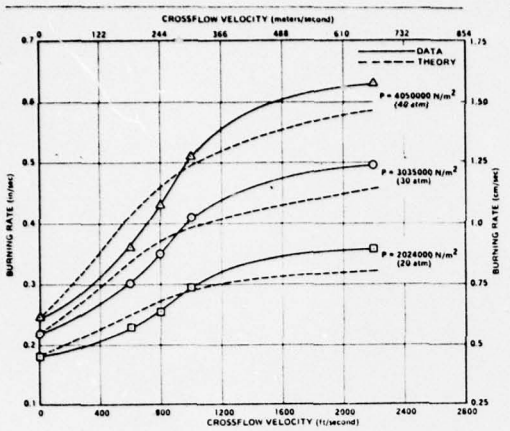

Figure 5. Burning-Rate Versus Crossflow Data and Predictions for Various Pressures for Formulation 4525 (73/27 AP/HTPB, 20μm AP).

Summary

Past modeling efforts in the area of erosive burning of solid propellants have been reviewed and lack of a model which incorporates a realistic description of composite propellant combustion has been noted. A possible physical mechanism by which cross flows may affect the combustion of a composite propellant has been postulated and a mathematical model for prediction of the burning rate of a composite propellant in such a crossflow, given only the no-crossflow burning rate versus pressure characteristics of the propellant, has been developed. This model has been used to predict remarkably well the erosive burning characteristics of a propellant studied by Saderholm. In addition, reasonable agreement between predictions and data has been obtained for a formulation recently characterized in our test facility. Additional propellants are currently being studied, and erosive burning rate data and predictions for these formulations will be compared for these formulations for further testing of the model in the near future. In addition, a second generation model based on this same picture which does not require no-crossflow burning rate versus pressure data but instead uses only propellant composition and ingredient size as input is currently under development.

Nomenclature

A_2	constant given by Equation 17
A_3, A_4, A_5	empirical constants relating zero crossflow burning rate to pressure, obtained by regression analysis of data
b	pre-exponential in Vielle's burning rate law
c_p	average propellant heat capacity
d_p	oxidizer particle diameter
D	characteristic length for calculation of Reynold's Number
f	friction factor
G	crossflow mass flux
k_1, k_2	constants defined by Equation 5
k_3	erosivity constant in expression of form, $r/r_o = 1 + K_3 M$
K_1, K_2, K_3	constants relating standoff distances to pressure and burning mass flux, given by Equations 14-16
K_1'-----K_9'	grouped constants defined by Eqns. 26 - 33
L_{Diff}	diffusion distance (Figure 1)
L_{Kin}	distance associated with oxidizer/fuel reaction subsequent to mixing (Figure 1)
L_I	distance associated with oxidizer monopropellant reaction (Figure 1)
M	crossflow Mach Number
MW	molecular weight of propellant product gases
$\dot{m}$	propellant burning mass flux (linear burning rate x propellant density)
n	exponent in Vielle's burning rate law
P	Pressure
$\dot{q}_{feedback}$	heat feedback flux from gas flames to propellant surface
Q_{VAP}	heat per unit mass involved in various endothermic processes at or below the propellant surface, e.g., binder pyrolysis or AP sublimation.
Q_{AX}	heat per unit mass involved in various exothermic processes at or below the propellant surface.
R	gas law constant
r	linear burning rate
r_o	linear burning rate at zero crossflow
r_e	erosive contribution to linear burning rate ($r - r_o$)
r_{aft}	linear burning rate of aft end of a grain port
r_{fore}	linear burning rate at fore end of a grain port
Re	Reynolds Number
T_{AP}	ammonium perchlorate flame temperature
T_f	propellant flame temperature
T_s	propellant surface temperature
T_o	propellant bulk temperature
$T_{core\ gas}$	temperature of core gas flowing past a propellant surface
U*	friction velocity (shear velocity) of crossflow
$U_{Mainstream}$	mainstream crossflow velocity
$U_{Crossflow}$	local crossflow velocity at a given distance from the propellant surface
$V_{Transpiration}$	blowing velocity of gases produced by propellant combustion normal to the surface, evaluated at the final flame temperature
Y, y	distance from propellant surface
Y^+	dimensionless distance, $\rho_{gas} U^* Y / \mu_{gas}$
γ	specific heat ratio of propellant product gases

λ_A, λ_B	gas thermal conductivity, with an area ratio term for each flame included
ρ_{gas}	propellant product gas density
ρ_s	solid propellant density
θ	angle between propellant surface and vector resultant of crossflow and transpiration velocities. (Figure 1)
τ_1	characteristic reaction time for AP monopropellant reaction
μ, μ_{gas}	propellant product gas viscosity.

References

1. King, M.K., "Effects of Crossflow on Solid Propellant Combustion: Interior Ballistic Design Implications", 1976 JANNAF Propulsion Meeting, Atlanta, GA., Dec., 1976. CPIA Publication 280, Vol. V, p. 341

2. Viles, J.M. "Prediction of Rocket-Motor Chamber Pressures Using Measured Erosive-Burning Rates," Technical Report S-275 (Contract DAAH01-70-C-0152) Rohm and Haas Co., Huntsville, Alabama 35807, October, 1970. CONFIDENTIAL

3. Saderholm, C.A., "A Characterization of Erosive Burning for Composite H-Series Propellants," AIAA Solid Propellant Rocket Conference, Palo Alto, California, January 29, 1964.

4. Kreidler, J.W., "Erosive Burning: New Experimental Techniques and Methods of Analysis," AIAA Solid Propellant Rocket Conference, Palo Alto, California, January 29, 1964.

5. Schultz, R., Green, L., and Penner, S.S., "Studies of the Decomposition Mechanism, Erosive Burning, Sonance and Resonance for Solid Composite Propellants," Combustion and Propulsion, 3rd AGARD Colloquium, Pergamon Press, N.W., 1958.

6. Green, L., "Erosive Burning of Some Composite Solid Propellants," Jet Propulsion, 24, 9, 1954.

7. Peretz, A., "Experimental Investigation of the Erosive Burning of Solid Propellant Grains with Variable Port Area," AIAA Journal, 6, 910, 1968.

8. Marklund, T., and Lake, A., "Experimental Investigation of Propellant Erosion, ARS Journal, 30, 173, 1960.

9. Dickinson, L.A., Jackson, F., and Odgers, A.L., "Erosive Burning of Polyurethane Propellants in Rocket Engines," Eighth Symposium (International on Combustion, 754, Williams and Wilkins, Baltimore, 1962.

10. Zucrow, M.J., Osborn, J.R., and Murphy, J.M., "An Experimental Investigation of the Erosive Burning Characteristics of a Nonhomogeneous Solid Propellant," AIAA Journal, 3, 523, 1965.

11. Vilyunov, V.N., Dvoryashin, A.A., Margolin, A.D., Ordzhonikidze, S.K., and Pokhil, P.F., "Burning of Ballistite Type H in Sonic Flow," Fizika Goreniya i Vzryva, 8, 4, 501-5, October - December, 1972.

12. Lenoir, J.M., and Robillard, G., "A Mathematical Method to Predict the Effects of Erosive Burning in Solid-Propellant Rockets," Sixth Symposium (International) on Combustion, 663 Reinhold Publishing Corp., New York, 1957.

13. Burick, R.J. and Osborn, J.R., "Erosive Combustion of Double-Base Solid Rocket Propellants", 4th ICRPG Combustion Conference, CPIA Publication 162, Vol. II, pp57-69, Dec., 1967.

14. Zucrow, M.J., Osborne, J.R., and Murphy, J.M., "The Erosive Burning of a Nonhomogeneous Solid Propellant," AICHE Symposium Series No. 52, 23-29, 1964.

15. Jojic, B., and Blagojevic, D. J., "Theoretical Prediction of Erosive Burning Characteristics of Solid Rocket Propellant Based on Burning Rate Dependence of Pressure and Initial Temperature and its Energetic Characteristics", AIAA/SAE 12th Propulsion Conference, Palo Alto, Calif., July, 1976, AIAA Paper No. 76-697.

16. Saderholm, C.A., Biddle, R.A., Caveny, L.H., and Summerfield, M., "Combustion Mechanisms of Fuel Rich Propellants in Flow Fields," AIAA/SAE 8th Joint Propulsion Specialist Conference, New Orleans, Louisiana, November 29, 1972, AIAA Paper No. 72-1145.

17. Lengelle, G., "Model Describing the Erosive Combustion and Velocity Response of Composite Propellants," AIAA Journal, 13, 3, 315-322 March, 1975.

18. Corner, J., Theory of the Interior Ballistics of Guns, John Wiley and Sons, Inc., New York, 1950.

19. Vandenkerckhove, J., "Erosive Burning of a Colloidal Solid Propellant," Jet Propulsion, 28, 599, 1958.

20. Zeldovich, Y.B., "Theory of Propellant Combustion in a Gas Flow," Fizika Goreniya i Vzryva, 7, 4, 463-76, October - December, 1971.

21. Geckler, R.E., et al., Aerojet Engineering Corporation Report 445, 1950.

22. Tsuji, H., "An Aerothermochemical Analysis of Erosive Burning of Solid Propellant," Ninth International Symposium on Combustion, 384-393, 1963.

23. Beddini, R.A., Varma, A.K., and Fishburn, E.S., "A Preliminary Investigation of Velocity-Coupled Erosive Burning," 13th JANNAF Combustion Meeting, Monterey, Calif., Sept., 1976, CPIA Publication 281, Vol. II, p.385.

24. Kuo, K.K., Razdan, M.K., and Kovalcin, R.L., "Theoretical and Experimental Investigation of Erosive Burning of Non-Metalized Composite Solid Propellants," Presented at 1977 Joint AFOSR/AFRPL Rocket Propulsion Research Meeting, Lancaster, Calif., March, 1977.

25. Klimov, A.M., "Erosive Burning of Propellants," Combustion, Explosion, and Shock Waves, 11,

5, Oct., 1976, p. 678.

26. Molnar, O., "Erosive Burning of Propellant Slabs," AIAA/SAE 8th Joint Propulsion Specialist Conference, New Orleans, LA., Nov. 1972, AIAA Paper 72-1108.

27. Miller, E., "Erosive Burning of Composite Solid Propellants," Combustion and Flames, Vol. 10, p. 330, Dec., 1966.

28. King, M., "A Modification of the Composite Propellant Erosive Burning Model of Lenoir and Robillard," Combustion and Flame, 24, 365-368, 1975.

29. Mickley, H.S., and Davis, R.S., "Momentum Transfer for Flow Over a Flat Plate with Blowing," NACA Technical Note 4017, November, 1957.

30. Sutherland, G.S., "The Mechanism of Combustion of an Ammonium Perchlorate-Polyester Resin Composite Solid Propellant," Ph.D. Thesis, Princeton, 1956.

31. King, M., "Erosive Burning of Composite Propellants," 13th JANNAF Combustion Meeting, Monterey, Calif., Sept., 1976, CPIA Publication 281, Vol. II, p. 407.

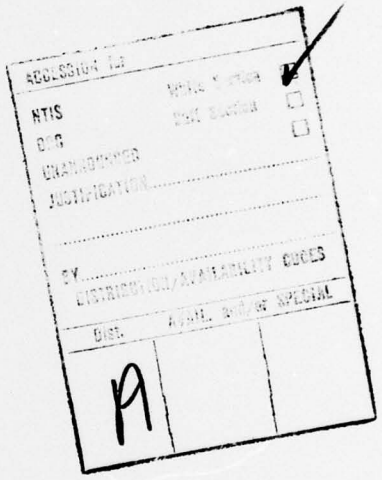

SECURITY CLASSIFICATION OF THIS PAGE *(When Data Entered)*

REPORT DOCUMENTATION PAGE

READ INSTRUCTIONS BEFORE COMPLETING FORM

1. REPORT NUMBER: AFOSR-TR-77-0692	2. GOVT ACCESSION NO.
3. RECIPIENT'S CATALOG NUMBER	
4. TITLE *(and Subtitle)*: A MODEL OF EROSIVE BURNING OF COMPOSITE PROPELLANTS,	5. TYPE OF REPORT & PERIOD COVERED: INTERIM
	6. PERFORMING ORG. REPORT NUMBER
7. AUTHOR(s): MERRILL K. KING	8. CONTRACT OR GRANT NUMBER(s): F44620-76-C-0023
9. PERFORMING ORGANIZATION NAME AND ADDRESS: ATLANTIC RESEARCH CORPORATION, KINETICS & COMBUSTION GROUP, 5390 CHEROKEE, ALEXANDRIA, VA 22314	10. PROGRAM ELEMENT, PROJECT, TASK AREA & WORK UNIT NUMBERS: 2308A1, 61102F
11. CONTROLLING OFFICE NAME AND ADDRESS: AIR FORCE OFFICE OF SCIENTIFIC RESEARCH/NA, BLDG 410, BOLLING AIR FORCE BASE, D C 20332	12. REPORT DATE: 1977
	13. NUMBER OF PAGES: 10 (12 pp.)
14. MONITORING AGENCY NAME & ADDRESS *(if different from Controlling Office)*	15. SECURITY CLASS. *(of this report)*: UNCLASSIFIED
	15a. DECLASSIFICATION/DOWNGRADING SCHEDULE

16. DISTRIBUTION STATEMENT *(of this Report)*

Approved for public release; distribution unlimited.

17. DISTRIBUTION STATEMENT *(of the abstract entered in Block 20, if different from Report)*

18. SUPPLEMENTARY NOTES

19. KEY WORDS *(Continue on reverse side if necessary and identify by block number)*

EROSIVE BURNING
NOZZLELESS ROCKET MOTORS
CROSSFLOWS
PROPELLANT BURNING
COMPOSITE PROPELLANTS

20. ABSTRACT *(Continue on reverse side if necessary and identify by block number)*

Development of solid rocket motor designs which result in high velocity flows of product gases across burning propellant surfaces (notably, nozzleless rocket motors) is leading to increased occurrence of erosive burning. In this paper, a physically realistic picture of the effect of such crossflow on composite propellant combustion, based on the bending of columnar diffusion flames by the crossflow, is presented. This bending results in shifting of the diffusion flame heat release zone toward the surface, with consequent increased heat feedback flux from this flame to the surface and thus increased burning rate. A relatively simple analytical model based on this picture is developed for

DD FORM 1 JAN 73 1473 EDITION OF 1 NOV 65 IS OBSOLETE

UNCLASSIFIED

SECURITY CLASSIFICATION OF THIS PAGE *(When Data Entered)*

prediction of propellant burning rate as a function of pressure and crossflow velocity, given only zero-crossflow burning rate versus pressure data. Model predictions and experimental results are compared, with reasonably good agreement being found.